Available online at www.sciencedirect.com

ScienceDirect

Mendeleev Commun., 2021, **31**, 723–725

Mendeleev Communications

Synthesis and structure assignment of vanadyl(IV) citrate $[(VO)_3(C_6H_5O_7)_2]\cdot H_2O$

Inna V. Baklanova,* Viktor D. Zhuravlev, Alexander P. Tyutyunnik, Marina A. Melkozerova and Tatyana A. Patrusheva

Institute of Solid State Chemistry, Ural Branch of the Russian Academy of Sciences, 620990 Ekaterinburg, Russian Federation. E-mail: baklanova_i@ihim.uran.ru

DOI: 10.1016/j.mencom.2021.09.044

Pseudo-crystals of vanadyl(IV) citrate $[(VO)_3(C_6H_5O_7)_2]\cdot H_2O$ have been obtained after addition of V_2O_5 to citric acid solution. Composition of the compound has been established by thermal analysis and confirmed by IR, UV-VIS, Raman and ESR spectra.

Keywords: citric acid, vanadyl citrate, IR, Raman, ESR, absorption spectrum, DTA.

Vanadium oxides and other vanadium compounds find an application as catalysts, devices with the kagome lattice, lithium-ion cathode materials, gas sensors, intellectual thermochromic windows and supercapacitors.[1–8] They also possess insulin-like action combined with oral applicability for potential treatment of diabetes,[9,10] with only vanadyl chelates meeting the related pharmacokinetic and pharmacodynamics requirements.[10] Materials with different vanadium valences are typically prepared from chemically active precursors by the solvothermal route with following calcination[11,12] or by so-called solution combustion synthesis, which represents an exothermic redox reaction between metal salts as oxidants and urea, glycine or citric acid as a fuel.[13] Citric acid acts as well like a chelating agent, which allows one to use solutions with a high concentration of vanadium[13,14] in the form of vanadyl ion and adjust the morphology and crystal structure of the product in a desired manner. The vanadyl-based complexes are typically produced as solutions[15–18] starting from vanadyl sulfate[16] or VCl_3.[17] Vanadyl and alkaline metal citrates have been isolated in the crystalline form,[17] while there is no available data on the production of vanadyl citrate in a solid state.

In this work, vanadyl citrate $[(VO)_3(C_6H_5O_7)_2]\cdot H_2O$, compound **1**, was isolated from V_2O_5–citric acid monohydrate solution (1 : 2) after spontaneous partial crystallization at room temperature for 48 h. Following addition of V_2O_5, the citric acid solution was heated with stirring at 70–80 °C until the oxide was completely dissolved. Then the volume of the solution was reduced by 25% and a glass formed was cooled to room temperature. After 48 h a precipitate was produced and separated from the solution, washed twice with cooled distilled water and dried at 80 °C for 3 h in a desiccator. In a solid state, compound **1** represents dark-blue druses [Figure 1(*a*)] with appearance like a crystal aggregate, though the X-ray diffraction data revealed its amorphous (pseudo-crystalline) nature [Figure 1(*b*)].† Compound **1** was further characterized by thermal analysis as well as UV-VIS, IR, Raman and ESR spectroscopy.‡

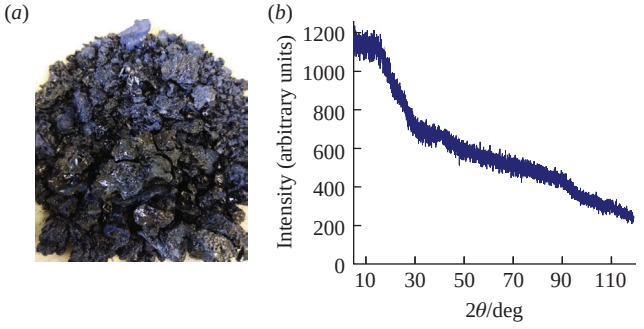

Figure 1 (*a*) Solid state druses and (*b*) X-ray powder diffraction data of compound **1**.

According to the thermal analysis results, the sample weight decreases in steps corresponding to two-stage decomposition of the $C_6H_5O_7^{3-}$ anions [Figure 2(*a*)]. In the range 80–190 °C, the weight decreases by 11.8% due to the loss of crystallization water and beginning of the oxidation of citrate ion. Further heating to 380 °C leads to the weight loss of 31.8%, which corresponds to decay of one of the two $C_6H_5O_7^{3-}$ anions, the related calculated

† X-ray powder diffraction investigation was performed at room temperature with CuKα_1 radiation using a STADI-P powder diffractometer (STOE) equipped with a mini position sensitive detector (PSD) in transmission geometry and scanning step $\Delta 2\theta = 0.02°$, $2° \leqslant 2\theta \leqslant 120°$.

‡ Thermal analysis was carried out using an STA 449 F3 Jupiter synchronic thermal analysis facility (NETZSCH) in alundum crucibles at 30–600 °C and 10 °C min^{-1}. The measurement cell with a sample was blown with air at a rate of 20 ml min^{-1}. The data obtained were processed using a NETZSCH Proteus software.

UV-VIS absorption spectrum, including NIR range, was recorded on a UV-2600 spectrophotometer (Shimadzu) with $BaSO_4$ as a standard.

IR spectrum in the range 4000–400 cm^{-1} was recorded on a Vertex 80 IR Fourier spectrometer (Bruker) using an MVP-Pro ATR accessory with a diamond crystal (Harrick Scientific).

Raman spectra were obtained at room temperature in the range 100–4000 cm^{-1} using an inVia Reflex confocal Raman microscope (Renishaw) with excitation by laser at λ = 532 nm and laser power values of 1 and 5 mW.

ESR spectrum was recorded at room temperature in the X-band on a standard CMS 8400 spectrometer (ADANI).

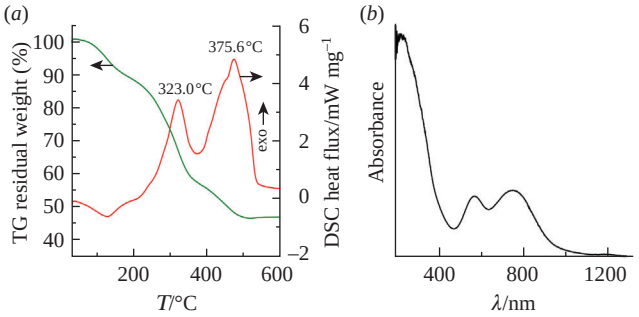

Figure 2 (*a*) Thermal analysis data and (*b*) absorption spectrum of compound **1**.

amount being 31.66%. Further decomposition of compound **1** occurs simultaneously with oxidation of VO_2 to V_2O_5 with the weight decrease by 10.5%. The degradation of citrate ion is accompanied by its oxidation, as indicated by exothermal peaks on the DSC curve [see Figure 2(*a*)]. X-ray powder diffraction analysis of the sample after calcination revealed the formation of V_2O_5. The residual weight comprises 46.9%, which agrees well with the mass loss upon calcination of a 3 g sample at 500 °C (54.29%). These data confirm the empirical formula of compound **1** as $[(VO)_3(C_6H_5O_7)_2]\cdot H_2O$ and correspond to the following equation of thermal decomposition:

$$4[(VO)_3(C_6H_5O_7)_2]\cdot H_2O + 39O_2 \rightarrow 6V_2O_5 + 48CO_2 + 24H_2O. \quad (1)$$

The absorption spectrum of compound **1** in the ultraviolet, visible and near infrared ranges [Figure 2(*b*)] reveals the following. Vanadium in the sample is in the form of vanadyl ion VO^{2+}, for which the typical octahedral environment is known. In tetragonal symmetry, the ground level T_{2g} splits into the $^2B_{2g}$ and ^2E_g ones, while the excited level ^2E_g splits into the $^2B_{1g}$ and $^2A_{1g}$ ones.[19,20] Thus, the absorption spectrum of VO^{2+} ion has three bands corresponding to the electronic *d*–*d* transitions of vanadium(IV) ion, namely $^2B_{2g}\rightarrow{}^2E_g$ (~1200 nm), $^2B_{2g}\rightarrow{}^2B_{1g}$ (760 nm) and $^2B_{2g}\rightarrow{}^2A_{1g}$ (574 nm). An absorption band with a maximum at 220 nm attributed to the transition with oxygen–vanadium charge transfer is registered in the UV range. The absorption band edge value is 3.5 eV.

The IR spectrum of compound **1** (Figure 3) has a broad absorption band in the range 3400–3100 cm^{-1} responsible for the characteristic stretching vibrations of water (Table 1). The stretching vibrations of C–H bonds manifest themselves as a set of bands in the range 2950–2800 cm^{-1}. The absorption band at 960 cm^{-1} corresponds to the stretching vibrations of the vanadyl group V^{4+}=O. Bands at 1629 and 1542 cm^{-1} as well as 1419 and 1360 cm^{-1} are responsible for the asymmetrical and symmetrical COO^- stretching vibrations, respectively. The symmetrical stretching vibrations of the COO^- groups are superimposed on the bending ones for the C–H bond. Absorption at 1213 cm^{-1} belongs to the asymmetrical stretching vibrations of the =C–O bond. The bands

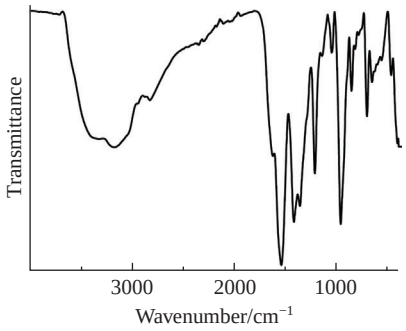

Figure 3 IR spectrum of compound **1**.

Table 1 Assignment of IR and Raman data for compound **1**.

IR modes/ cm^{-1}	Raman modes/ cm^{-1}	Assignment	IR modes/ cm^{-1}	Raman modes/ cm^{-1}	Assignment
3329	3464	ν H_2O	1143	1138	ν C–O
3178			1048	1069	
2947	3005	ν C–H		966	ν V=O
2830	2927		960	885	
1629	1572	ν_{as} COO	854	855	ν C–C
1542			819		
1419	1425	ν_s COO	784	748	δ OCO
1360			703		δ C–H
	1284	δ C–H	653	627	δ C–C
	1232		560		δ C–C
1213		ν =C–O	465		δ OCO

at 1143 and 1048 cm^{-1} result from vibrations of the C–O bond. The bands with maxima at 854 and 819 cm^{-1} are attributed to the stretching vibrations of C–C bonds, and those at 653 and 560 cm^{-1} to the bending vibrations. The band with the absorption maximum at 784 cm^{-1} corresponds to the scissors vibration of COO^-. The band with frequency 703 cm^{-1} is related to the pendular bending vibrations of C–H. The band at 465 cm^{-1} is due to the out-of-plane bending vibrations of COO^-.

The Raman spectrum of compound **1** at a laser power of 1 mW (Figure 4, spectrum *1*) is in accordance with its IR spectrum. The lines at 1284 and 1232 cm^{-1} correspond to planar bending vibrations of the C–H bonds. Raman lines of multiple V=O bonds are split into two components, namely the ones at 966 and 885 cm^{-1}. For the complete assignment of the IR and Raman modes, see Table 1. When the laser power applied was increased to 5 mW, compound **1** began to break down and the color of the sample in the laser exposure point changed from blue to orange, as a result the spectrum of vanadium(V) oxide was obtained (Figure 4, spectrum *2*) with modes at 989, 687, 512, 464, 404, 282, 190 and 138 cm^{-1} in agreement with the corresponding orthorhombic structure. The lines at 138 and 190 cm^{-1} are related to the lattice vibrations of vanadium oxide. The peaks located at 282 and 404 cm^{-1} are responsible for the bending vibrations of (V=O) bond. The bending vibrations of (V–O–V) are observed at 464 cm^{-1}. The line at 512 cm^{-1} is attributed to the stretching vibrations of tri-coordinated oxygen (V_3–O). The stretching vibrations of double-coordinated oxygen (V_2–O) are registered at 687 cm^{-1}. The high-frequency mode at 989 cm^{-1} is due to the stretching vibrations of end atoms of oxygen (V=O).

An intense Lorentzian line shape signal at g = 1.974 is registered in the ESR spectrum of compound **1** (Figure 5). The g-value corresponds to the reference data for V^{4+} ($3d^1$).[21] The large linewidth ΔH_{p-p} = 360 G indicates a low degree of crystallinity of the obtained sample.

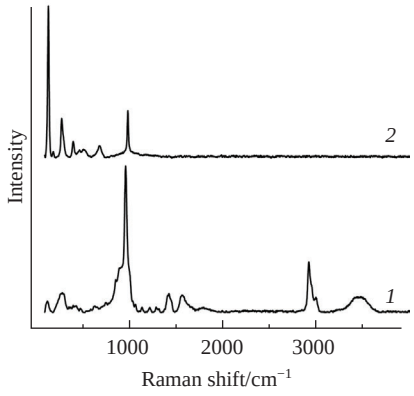

Figure 4 Raman spectra of (*1*) compound **1** and (*2*) V_2O_5.

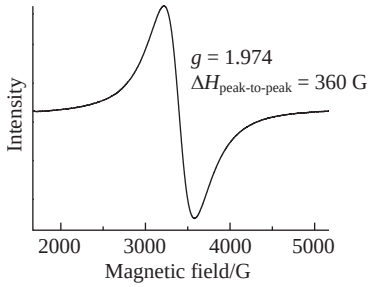

Figure 5 ESR spectrum of compound **1**.

In summary, the structure of pseudo-crystalline precipitate separated from saturated citric acid solution after dissolution of vanadium(V) oxide has been determined. According to X-ray diffraction data, the material is amorphous. IR, Raman, UV-VIS and ESR spectra confirm the formation of vanadyl cation VO^{2+}. The compound was described as monohydrous triple-substituted vanadyl citrate $[(VO)_3(C_6H_5O_7)_2]\cdot H_2O$.

This work was carried out in accordance with the State Assignment of the Institute of Solid State Chemistry, Ural Branch of the Russian Academy of Sciences (grants nos. AAAA-A19-119031890026-6 and AAAA-A19-119031890025-9). The absorption spectrum was recorded in the Center for Joint Use 'Spectroscopy and Analysis of Organic Compounds' at the I. Ya. Postovsky Institute of Organic Synthesis, Ural Branch of the Russian Academy of Sciences.

References

1 Y. Zhang, C. Chen, W. Wu, F. Niu, X. Liu, Y. Zhong, Y. Cao, X. Liu and C. Huang, *Ceram. Int.*, 2013, **39**, 129.
2 S. Milošević, I. Stojković, S. Kurko, J. G. Novaković and N. Cvjetićanin, *Ceram. Int.*, 2012, **38**, 2313.
3 I. P. Parkin and T. D. Manning, *J. Chem. Educ.*, 2006, **83**, 393.
4 Z. Liang, Y. Zhao, L. Ouyang, Y. Dong, Q. Kuang, X. Lin, X. Liu and D. Yan, *J. Power Sources*, 2014, **252**, 244.
5 P. A. Deshpande and G. Madras, *AIChE J.*, 2011, **57**, 2215.
6 K. Fritsch, M. Ramazanoglu, H. A. Dabkowska and B. D. Gaulin, *J. Cryst. Growth*, 2011, **327**, 205.
7 V. Soundharrajan, B. Sambandam, J. Song, S. Kim, J. Jo, S. Kim, S. Lee, V. Mathew and J. Kim, *ACS Appl. Mater. Interfaces*, 2016, **8**, 8546.
8 M.-C. Liu, L.-B. Kong, L. Kang, X. Li, F. C. Walsh, M. Xing, C. Lu, X.-J. Ma and Y.-C. Luo, *J. Mater. Chem. A*, 2014, **2**, 4919.
9 A. Gorzsás, *PhD Thesis*, Umeå, Sweden, 2005.
10 M. W. Makinen and M. Salehitazangi, *Coord. Chem. Rev.*, 2014, **279**, 1.
11 J. Liu, Y. Zhou, J. Wang, Y. Pan and D. Xue, *Chem. Commun.*, 2011, **47**, 10380.
12 H. Li, J. Wang, X. Liu, Q. Sun, A. B. Djurišić, M. Xie, Y. Mei, C. Y. Tang and K. Shih, *RSC Adv.*, 2017, **7**, 2480.
13 H. Wu, M. Qin, Z. Cao, X. Li, B. Jia, P. Chen, M. Huang and X. Qu, *Chem. Phys. Lett.*, 2018, **706**, 7.
14 N. Van Landschoot, E. M. Kelder and J. Schoonman, *J. Solid State Electrochem.*, 2003, **8**, 28.
15 N. Peys, P. Adriaensens, S. Van Doorslaer, S. Gielis, E. Peeters, C. De Dobbelaere, S. De Gendt, A. Hardy and M. K. Van Bael, *Dalton Trans.*, 2014, **43**, 12614.
16 S. Berto, P. G. Daniele, E. Diana, E. Laurenti and E. Prenesti, *Inorg. Chim. Acta*, 2014, **414**, 105.
17 M. Tsaramyrsi, M. Kaliva, A. Salifoglou, C. P. Raptopoulou, A. Terzis, V. Tangoulis and J. Giapintzakis, *Inorg. Chem.*, 2001, **40**, 5772.
18 M. Tsaramyrsi, D. Kavousanaki, C. P. Raptopoulou, A. Terzis and A. Salifoglou, *Inorg. Chim. Acta*, 2001, **320**, 47.
19 C. J. Ballhausen and H. B. Gray, *Inorg. Chem.*, 1962, **1**, 111.
20 B. P. Maurya, A. Punnoose, M. Umar and R. J. Singh, *Solid State Commun.*, 1994, **89**, 59.
21 H. A. Kuska and M. T. Rogers, *Electron Spin Resonance of First Row Transition Metal Complex Ions*, Interscience, New York, 1968.

Received: 5th April 2021; Com. 21/6515